Interaction of Nonideal, Multicomponent Solid Solutions With Water: A Simple Algorithm to Estimate Final Equilibrium States

R. M. Rodríguez-Galán[1] (ID) **and M. Prieto[1]** (ID)

[1]Departamento de Geología, Universidad de Oviedo, C/Arias de Velasco, Oviedo, Spain

Abstract Interaction of minerals with water frequently yields a dissolution-coprecipitation process in which foreign ions incorporate into the solid structure substituting for the major ion. Coprecipitation often controls the transport and fate of harmful ions in the environment. Geochemical modeling and experimental studies of these aqueous-solid solution (AQ-SS) processes are typically performed using pure minerals. However, the host minerals could be binary solid solutions and the study of their interaction with a third dissolved ion would require considering ternary solid solutions (TSS). Here we present a simple algorithm (AQ-TSS) implemented in PHREEQC to estimate equilibrium in AQ-SS systems involving nonideal ternary solid solutions. The three binary joints are considered separately. Nonregular solid solutions are treated by combining regular models defined for specific ranges of composition. The algorithm has been tested successfully by comparing the results obtained by AQ-TSS with those obtained using PHREEQC with the same binary nonideal solid solutions.

1. Introduction

The interaction of primary minerals with water frequently yields a dissolution-precipitation process in which minor elements incorporate into structural positions forming solid solution with the host mineral. In this way, carbonates and other moderately soluble minerals frequently control the transport, fate, and impact of metals in the environment, producing a "natural attenuation" in some polluted areas. Aqueous-solid solution (AQ-SS) processes can be used in "active" remediation measures to immobilize toxic metals, radionuclides, and other harmful ions generated by human activities. Because structural incorporation is generally a more durable retention mechanism than adsorption or ionic exchange, AQ-SS systems have attracted increasing attention from environmental scientists and engineers during the last decades (Bruno et al., 2007; Curti, 1997; Fernández-González et al., 2013; Godelitsas & Astilleros, 2010; Noguera et al., 2012; Prieto et al., 2013; Putnis, 2010; Zhang et al., 2014, and references there in).

Most experimental studies on the uptake of foreign ions by coprecipitation have been performed using pure samples of the host mineral, which implies considering a solid solution formed by two components, the pure host mineral and the equivalent pure compound of the guest ion. With some exceptions (Noguera et al., 2012; Vinograd et al., 2010; Wagner et al., 2012), geochemical modeling of AQ-SS processes deals with binary solid solutions and the same occurs with the experimental and atomistic estimation of thermodynamic nonideality parameters. However, in aquifers, soils, and other aquatic environments, the potential host minerals could be binary solid solutions and the study of their interaction with a third dissolved ion would require considering ternary solid solutions (TSS). In marine environments, skeletal calcite and calcite cements can incorporate amounts of about 15–20 mol % of $MgCO_3$ (Böttcher & Dietzel, 2010), whereas natural, inorganic calcites incorporate up to 2–3 mol % of magnesium. Manganese-rich calcites formed in marine and nonmarine environments are also very common (Katsikopoulos et al., 2009; Mucci, 2004). Natural barites ($BaSO_4$) contain up to about 7 mol % of $SrSO_4$ (Hanor, 2000; Monnin & Cividini, 2006) and many aragonites incorporate significant amounts of strontium in their structure. Thinking in "active" remediation measures, the relevant question is whether the effectiveness in removing a given ion from water could increase using a solid solution instead of the pure mineral (Prieto et al., 2016). Unfortunately, there is no simple answer to this question. A significant increase of effectiveness has been observed in a comparative study on the uptake of Pb^{2+} by pure barite and Sr-bearing barite (Prieto et al., 2014). In contrast, the removal of radium by interaction with either (Sr, Ba)SO_4 or pure barite seems to be similar (Zhang et al.,

2014). The effectiveness can depend, among other factors, on: (i) the specific guest ion-SS system, (ii) the initial composition of both the solid and the aqueous solution, (iii) the relative amount of solid and fluid involved in the reaction, and (iv) kinetic and mechanistic effects that can operate at different scales in space and time (Prieto et al., 2016).

All these factors need to be considered from a thermodynamic and kinetic perspective. AQ-SS systems require ongoing dissolution-crystallization to approach equilibrium and may need a long time to form a combination of compositionally homogeneous solid phases at equilibrium with the remaining aqueous solution. However, the first step in modeling coprecipitation processes is providing the equilibrium state to which a specific AQ-SS system will tend to react (Glynn et al., 1990). Such an equilibrium state is the output of the solid-solution tool of PHREEQC (Parkhurst & Appelo, 2013), which is a well-known computer code that enables a wide variety of calculations. The keyword "SOLID SOLUTIONS" allows operating with nonideal binary solid solutions or ideal solid solutions with any number of components. However, PHREEQC does not deal with nonideal ternary or higher order solid solutions. As far as we know, GEM-Selektor (Kulik et al., 2013; Wagner et al., 2012) is the only modeling code that allows calculating equilibrium in AQ-SS systems that involve nonideal multicomponent solid solutions. Other codes such as GWB (Bethke & Yeakel, 2017), MINTEQA2 (Allison et al., 1991), and EQ3/6 (Wolery, 1992) do not deal with solid solutions. Differently from PHREEQC, GWB, etc., GEM-Selektor is not based on the Law of Mass Action (LMA) formalism but on a Gibbs Energy Minimization (GEM) algorithm (Kulik et al., 2013). GEM can solve complex aqueous-solid equilibria in one run, without using the iterative procedures required in LMA speciation models. Moreover, in the case of AQ-SS systems, GEM can deal with ideal and regular solid solutions of high order.

Here we present a simple algorithm (AQ-TSS) that allows estimating AQ-SS equilibrium endpoints in the case of nonideal (regular, subregular, or any-type) ternary solid solutions. The (Pb, Sr, Ba)SO$_4$ solid solution is used as example system. We have implemented the algorithm to work in a PHREEQC context via the BASIC interpreter tool of this "popular" modeling code. The extension to nonideal solid solutions of higher order is feasible but the formulations become bulkier with each added component.

2. Background

AQ-SS thermodynamics is a complex issue that generated many controversies during the past three decades (Glynn & Reardon, 1990; Prieto, 2009). Here to avoid misunderstandings, we review the basis, even at the risk of being too elementary. The dissolution of a stoichiometric mineral can be described by a dissociation reaction, which in the case of a hypothetical pure BA solid would be:

$$BA_{(s)} \longrightarrow B^+_{(aq)} + A^-_{(aq)} \tag{1}$$

where the subscripts s and aq stand for solid and aqueous, respectively. Applying the LMA formalism, the equilibrium condition would be:

$$K_{BA} = \frac{\{B^+\}\{A^-\}}{a_{BA}} \tag{2}$$

where the terms B^+ and A^- within curly brackets are the activities of the uncomplexed aqueous ions, a_{BA} is the activity of the component BA in the solid phase, and K_{BA} is the equilibrium constant for the reaction (1). The aqueous solution composition can be complex, but several models relate concentration to activity as a function of the ionic strength (Appelo & Postma, 2005). Consistently with PHREEQC, the standard state for aqueous species has been chosen to be a hypothetical ideal 1 molal aqueous solution. Thus, for the free (uncomplexed) B^+ ions:

$$\{B^+\} = \gamma_{B^+} \frac{[B^+]}{[B^+]^o} = \gamma_{B^+} [B^+] \tag{3}$$

where $[B^+]^o$ is the standard state concentration (1 mol/kg water), $[B^+]$ is the molal concentration of the aqueous B^+ ions, and γ_{B^+} is the corresponding aqueous activity coefficient. For solids, the standard state is the pure solid and a_{BA} is given by the expression:

$$a_{BA} = \gamma_{BA} \frac{X_{BA}}{X_{BA}^o} = \gamma_{BA} X_{BA} \tag{4}$$

where X_{BA} is the mole fraction of the component BA in the solid phase, $X_{BA}^o = 1$ represents the standard state, and γ_{BA} is a dimensionless activity coefficient of the component BA in the solid phase. In the case of a pure solid, equation (2) becomes:

$$K_{BA} = \{B^+\}\{A^-\} \tag{5}$$

because $a_{BA} = \gamma_{BA} = X_{BA} = 1$, and thus K_{BA} is termed thermodynamic solubility product.

In the case of a binary solid solution $(C,B)A$, the solid phase can be seen as consisting of two components, BA and CA, and the dissolution process requires two reactions to be described, one for each component of the solid solution. Therefore, two equilibrium conditions must be simultaneously satisfied, namely:

$$K_{BA} = \frac{\{B^+\}\{A^-\}}{a_{BA}} \tag{6a}$$

and

$$K_{CA} = \frac{\{C^+\}\{A^-\}}{a_{CA}} \tag{6b}$$

Equation (6a) is obviously identical to equation (2). K_{BA} and K_{CA} are the thermodynamic solubility products of the pure end-members BA and CA. The solid phase activities differ from unity for any intermediate $(0 < X_{BA} < 1)$ composition. Although in a binary solid solution the composition depends on a single variable $(X_{BA} = 1 - X_{CA})$, for the sake of displaying the equations in an effortless way, we will use both X_{BA} and X_{CA} in the formulations.

Checking whether a given AQ-SS system is at equilibrium only requires verifying that the equilibrium conditions for the end-members are concurrently fulfilled. Determining the equilibrium state to which a given AQ-SS system tends is not so straightforward (Glynn et al., 1990). In contrast to monocomponent solids, the final compositions at equilibrium depend on the initial solid/fluid ratio. Together with the LMA equations (6a) and (6b), the calculation requires an additional equation related to the conservation of the charge in the solid and two equations related to the conservation of mass of the solid-solution components, i.e.,

$$\left[A^-\right]^T - \left[A^-\right]_i^T = \left[B^+\right]^T - \left[B^+\right]_i^T + \left[C^+\right]^T - \left[C^+\right]_i^T \tag{7}$$

and

$$n_i X_{BA}^i + M_w \left[B^+\right]_i^T = n X_{BA} + M_w \left[B^+\right]^T \tag{8a}$$

$$n_i X_{CA}^i + M_w \left[C^+\right]_i^T = n X_{CA} + M_w \left[C^+\right]^T \tag{8b}$$

where M_w is the mass of water (kg), the terms in square brackets represent the molalities of the corresponding ions, and n is the number of moles of solid. The superscript or subscript i stands for initial, and the superscript T indicates total, analytical concentration (uncomplexed + complexed ions). In practice, all i-labeled terms and M_w are known, i.e., the initial total molalities of the aqueous ions, the initial number of moles of both components in the solid phase, and the mass of water. Therefore, we are dealing with a system of five equations (6a, 6b, 7, 8a, and 8b) and five unknowns: n, X_{BA}, $[A^-]^T$, $[B^+]^T$, and $[C^+]^T$. There is still a problem because equations (6a) and (6b) deal with activities, while equations (7), (8a), and (8b) deal with molalities of the uncomplexed aqueous ions and mole fractions of the solid components. Therefore, the iterative derivation of solutions for this set of equations requires independent knowledge of the activity coefficients. For the aqueous ions, γ_{B^+}, γ_{C^+}, and γ_{A^-} can be obtained from the analytical concentration using any aqueous speciation program. For the solid components, the activity coefficients can be obtained by fitting experimental values of the excess free energy of mixing (ΔG^E) to a suitable equation. ΔG^E represents the degree of nonideality and is given by the difference between the free energy of mixing (ΔG^M) of the actual solid solution and that of an equivalent ideal solid solution. A discussion about the experimental determination of thermodynamic mixing parameters can be found in Glynn (2000). The lack of reliable

Table 1
Relationships Between Nonideality Parameters for Subregular Solid Solutions

Parameters	Dimension	Symbol 1	Symbol 2
Guggenheim	Dimensionless	a_0	a_1
Guggenheim dimensionful	Joule/mole	$A_0 = a_0 RT$	$A_1 = a_1 RT$
Margules-Thompson-Waldbaum	Joule/mole	$W_{BC} = A_0 - A_1$	$W_{CB} = A_0 + A_1$
Guggenheim dimensionful	Joule/mole	$A_0 = (W_{BC} + W_{CB})/2$	$A_1 = (W_{CB} - W_{BC})/2$

values for these parameters is a major obstacle in modeling AQ-SS processes, but molecular simulation methods appear to be a good way to overcome that problem (Kulik et al., 2010; Wang et al., 2011). Provided the numerous reviews on solid-solution thermodynamics available in the literature, we are going to jump directly to the expressions of γ_{BA} and γ_{CA} obtained using a Guggenheim (1937) expansion series to fit $\Delta G^E - X_{BA}$ data, namely

$$\ln\gamma_{BA} = X_{CA}^2 [a_0 + a_1(3X_{BA} - X_{CA}) + a_2(X_{BA} - X_{CA})(5X_{BA} - X_{CA}) + \ldots] \tag{9a}$$

and

$$\ln\gamma_{CA} = X_{BA}^2 [a_0 - a_1(3X_{CA} - X_{BA}) + a_2(X_{CA} - X_{BA})(5X_{CA} - X_{BA}) + \ldots] \tag{9b}$$

The terms a_0, a_1, a_2, etc. are dimensionless fitting parameters. Uppercase parameters ($A_0 = a_0 RT$, etc.) expressed in Joules/mole are also frequently used (R is the gas constant and T is the absolute temperature). For ideal solid solutions $a_0 = a_1 = a_2 = \cdots = 0$ and, therefore, γ_{BA} and $\gamma_{CA} = 1$. When all fitting parameters but a_0 are zero, the solid solution is called regular, while the term subregular refers to a solid solution with nonzero a_0 and a_1. For regular and subregular solid solutions, Margules-type functions (Thompson & Waldbaum, 1969) are commonly used, particularly in high temperature petrology and geochemistry. A detailed presentation of the classical solid-solution thermodynamics can be found in several reviews (Ganguly, 2001; Ganguly & Saxena, 1987). Table 1 displays the equivalence between Guggenheim and Thompson-Waldbaum parameters for a subregular solid solution model. It is worth noting that any equation that fits properly the ΔG^E versus X_{BA} data can be used to determine the solid-phase activity coefficients, which are related to ΔG^E by the general expressions:

$$\ln\gamma_{BA} = \left(\Delta G^E + X_{CA}\frac{\partial \Delta G^E}{\partial X_{BA}}\right)/RT \tag{10a}$$

and

$$\ln\gamma_{CA} = \left(\Delta G^E - X_{BA}\frac{\partial \Delta G^E}{\partial X_{BA}}\right)/RT. \tag{10b}$$

Equations (10a) turn into equations (9a) when we fit the experimental values of ΔG^E to a Guggenheim expansion series, namely

$$\Delta G^E = X_{BA}X_{CA}\left[a_0 + a_1(X_{BA} - X_{CA}) + a_2(X_{BA} - X_{CA})^2 + \ldots\right]RT \tag{11}$$

It is worth noting that the activity coefficients depend on the solid-solution composition, $\gamma_{BA} = f(X_{BA}, X_{CA})$ and $\gamma_{CA} = f(X_{BA}, X_{CA})$, as shown in Figure 1 and equations (9a).

3. Equilibrium in Multicomponent AQ-SS Systems

3.1. Extending the Problem to Ternary Solid Solutions

As previously discussed, the aim of this work is determining the equilibrium state in AQ-SS systems in the case of multicomponent (single-site) solid solutions. For the sake of simplicity, we are going to deal with ternary $(D,C,B)A$ solid solutions. Introducing a third component, DA, in the AQ-SS system involves adding a third equilibrium equation and a third mass-balance equation to the set of equations (6) and (8a), i.e.,
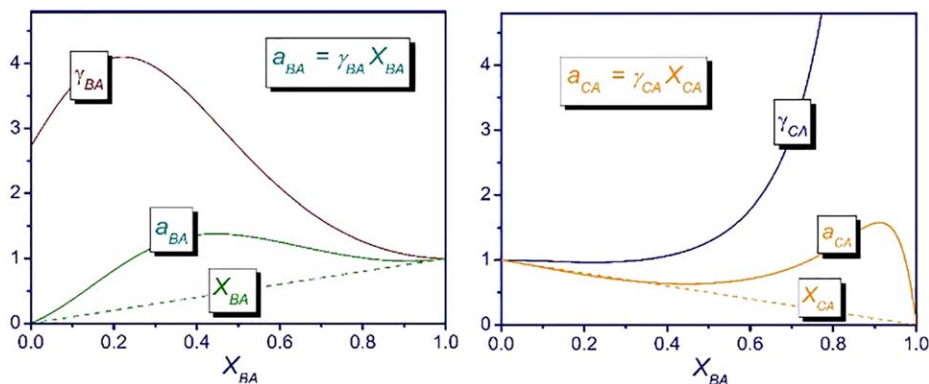
Figure 1. Variation of the activity coefficients γ_{BA} and γ_{CA} of the components of a hypothetical $(B,C)A$ solid solution. Note that in a binary solid solution $X_{BA} = 1 - X_{CA}$. Calculation performed for a subregular solid solution with $a_0 = 2.5$ and $a_1 = 1.5$.

$$K_{DA} = \frac{\{D^+\}\{A^-\}}{a_{DA}} \tag{12}$$

and

$$n_i X_{DA}^i + M_w \left[D^+\right]_i^T = n X_{DA} + M_w \left[D^+\right]^T \tag{13}$$

where K_{DA} is the thermodynamic solubility product of the pure DA end-member. Moreover, the charge-balance equation (7) becomes:

$$\left[A^-\right]^T - \left[A^-\right]_i^T = \left[B^+\right]^T - \left[B^+\right]_i^T + \left[C^+\right]^T - \left[C^+\right]_i^T + \left[D^+\right]^T - \left[D^+\right]_i^T. \tag{14}$$

This set of equations can be solved in the same way as in the case of a binary solid solution. However, ternary nonideal solid solutions are not implemented in PHREEQC (Parkhurst & Appelo, 2013), where it is only possible to model multicomponent solid solutions by considering them as ideal. Here our challenge is developing a tool for determining equilibrium states in AQ-TSS systems without introducing changes in the PHREEQC source code. With this aim, we can exploit the keyword data block of PHREEQC for ideal solid solutions. The scheme in Figure 2 shows the input and output for the hypothetical, ideal $(D,C,B)A$ solid solution.

3.2. The Algorithm

In the case of an ideal $(D,C,B)A$ solid solution, the activities of the components in the solid phase are equal to their mole fractions since the activity coefficients are equal to unity. Therefore, applying the ideal model to a nonideal solid solution we would obtain a value of the mole fraction that would differ from the actual value:

$$X_{BA_{id}} = \gamma_{BA} X_{BA_{real}}, \tag{15}$$

that is,

$$X_{BA_{real}} = X_{BA_{id}} / \gamma_{BA}. \tag{16}$$

for the BA component, where the subscripts id and $real$ refer to the ideal and real solid solutions, respectively. Unfortunately, the value of γ_{BA} depends on the solid-solution composition (X_{BA}, X_{CA}, X_{DA}) and we cannot directly apply equation (16) to calculate $X_{BA_{real}}$. However, we can solve this problem by means of an iterative procedure, according to the sequence:

$$\gamma_{BA}(I) = f[X_{BA}(I-1), X_{CA}(I-1), X_{DA}(I-1)] \tag{17a}$$

$$X_{BA}(I) = X_{BA}(I-1) / \gamma_{BA}(I-1). \tag{17b}$$

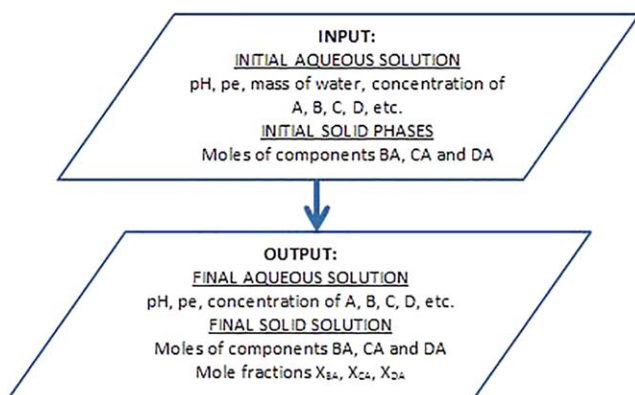Similarly, for the CA and DA components,

Figure 2. Input and output relevant data for determining equilibrium endpoints in AQ-SS systems.

$$\gamma_{CA}(I) = f[X_{CA}(I-1), X_{BA}(I-1), X_{DA}(I-1)] \tag{18a}$$

$$X_{CA}(I) = X_{CA}(I-1)/\gamma_{CA}(I-1) \tag{18b}$$

and

$$\gamma_{DA}(I) = f[X_{DA}(I-1), X_{CA}(I-1), X_{BA}(I-1)] \tag{19a}$$

$$X_{DA}(I) = X_{DA}(I-1)/\gamma_{DA}(I-1) \tag{19b}$$

where the starting value would be $X_{BA}(1) = X_{BA_{id}}$ and the index I will run from 2 until convergence. Although the composition of a ternary solid solution requires two variables to be described, we will use the three molar fractions (X_{BA}, X_{CA}, and X_{DA}) in the formulations. In practice, the three components BA, CA, and DA need to be included in a single iterative routine. We can use $cp = |X_{BA}(I) - X_{BA}(I-1)|$ as convergence parameter. Values of $cp < 10^{-5}$ are suitable in most cases, but we can reduce the tolerance when one of the components occurs at very trace concentrations. In general, less than 10 iterations are enough to reach convergence and determining $X_{BA_{real}}$ and γ_{BA}. Finally, we can consider the actual SS as an equivalent ideal SS in which the nonideality coefficients γ_{BA}, γ_{CA}, and γ_{DA} are incorporated to the solubility products of the end-members. With this aim, we need to define three "hypothetical" (h) pure end-members with the keyword PHASES of PHREEQC:

$$K_{BA_h} = K_{BA}\gamma_{BA}, \tag{20a}$$

$$K_{CA_h} = K_{CA}\gamma_{CA} \tag{20b}$$

and

$$K_{DA_h} = K_{DA}\gamma_{DA}. \tag{20c}$$

It is worth noting that these hypothetical solubility products depend on the specific composition of the solid solution, since the activity coefficients do.

3.3. Formulations of Activity Coefficients for Ternary Solid Solutions

Extending the activity coefficient formulations to ternary and quaternary solid solutions is feasible (Ganguly & Saxena, 1987; Mukhopadhyay et al., 1993), but many fitting parameters are needed (Anderson, 2005) and not many solid solutions have been investigated in this respect. Here we use the activity-coefficient functions for a ternary, symmetric solid solution (Zhu, 2004), i.e.,

$$\ln\gamma_{BA} = a_0^{BC}X_{CA}^2 + a_0^{BD}X_{DA}^2 + (a_0^{BC} - a_0^{CD} + a_0^{BD})X_{CA}X_{DA} \tag{21a}$$

$$\ln\gamma_{CA} = a_0^{BC}X_{BA}^2 + a_0^{CD}X_{DA}^2 + (a_0^{BC} - a_0^{BD} + a_0^{CD})X_{BA}X_{DA} \tag{21b}$$

$$\ln\gamma_{DA} = a_0^{BD}X_{BA}^2 + a_0^{CD}X_{CA}^2 + (a_0^{BD} - a_0^{BC} + a_0^{CD})X_{BA}X_{CA} \tag{21c}$$

where a_0^{BC}, a_0^{BD}, and a_0^{CD} are the three dimensionless nonideality parameters of the corresponding (binary and regular) solid solutions.

Modeling asymmetric, ternary solid solutions requires 2×3 binary-interaction parameters and an additional factor for ternary interactions (Mukhopadhyay et al., 1993). However, to simplify the formulations, we can divide the binary joints into several relevant composition ranges. For example, subregular, binary solid solutions can be treated by combining two regular solution models, each one for a compositional range starting in one of the end-members (Ganguly & Saxena, 1987; Zhu, 2004). Thus, in dealing with asymmetric ternary solid solutions, a set of 2×3 regular models can be combined, keeping in mind that such a treatment assumes that the contribution of ternary interactions is not very significant. This assumption is typical in most works on mineral solid solutions and is realistic when two of the three components occur in minor amounts. Hillert (1980) and Ganguly (2001) review the methods proposed in the fields of petrology and materials science to account for ternary interactions in solid solutions with wide ranges of miscibility. This topic is, however, beyond the scope of the present work. Here we focus on the development of an implementation (AQ-TSS) thought to model mineral-water interactions under conditions of temperature in which most of the relevant solid solutions exhibit limited ranges of miscibility. The miscibility limits are determined by the common tangent to the minima of the free energy of mixing (ΔG^M) function (Putnis et al., 1992) and can be calculated from the thermodynamic formulation, when the nonideality (a_0, a_1,...) parameters are known (see, for example, Figure 3).
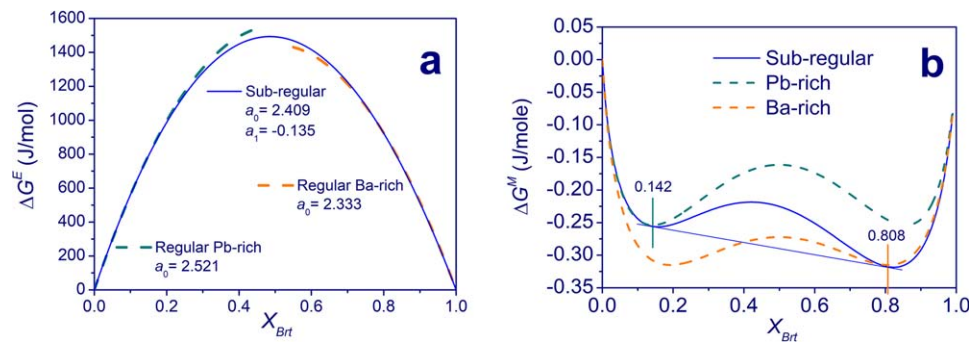
Figure 3. (a) $\Delta G^E(X_{Brt})$ function for the barite-anglesite solid solution calculated using a subregular ($a_0 = 2.409$ and $a_1 = -0.135$) model or a combination of two regular models. (b) Free energy of mixing of the barite-anglesite solid solution. The subregular model implies the presence of an asymmetric miscibility gap given by the common tangent to the two minima of the $\Delta G^M(XBrt)$ function (at 0.142 and 0.808). This curve is a combination of two regular functions, for the Ba-rich ($a_0 = 2.333$) and Pb-rich ($a_0 = 2.521$) halves of the series.

4. Algorithm Testing Using Case Studies

4.1. Regular Binary Solid Solutions: The Barite-Celestine Joint

PHREEQC works with binary regular and subregular solid solutions, which can be used to test the algorithm described in section 3.2. With this aim, we have chosen the barite (Brt)-celestine (Clt) solid solution. The complete (Ba, Sr)SO$_4$ series can be obtained experimentally at room temperature, but its mixing properties have been largely controverted in the literature (Zhu, 2004). In general, this solid solution is considered nearly regular, although different values for the dimensionless Guggenheim parameter have been proposed. Here we use a regular model with $a_0 = 2.3$ at 25°C as proposed by Glynn (2000). Such a model is consistent with a symmetric miscibility gap ($0.2 \lesssim X_{Clt} \lesssim 0.8$), which separates two miscibility ranges. Table 2 displays a comparison between the outputs obtained using the PHREEQC tool for binary nonideal solid solutions, AQ-TSS, and an ideal SS model (the specific AQ-TSS program is included with the supporting information; for $cp < 10^{-5}$ convergence was attained after six iterations). As can be seen, there is a significant difference between the aqueous concentrations obtained with the ideal model and the other two. The data estimated by AQ-TSS and PHREEQC differ less than 1%, which is negligible in comparison with other sources of uncertainty that are usual in these types of models. For output compositions that fall within the miscibility gap, the concentrations of barium and strontium within the aqueous phase remain fixed, but the aqueous phase is in equilibrium with solids of two compositions, each one corresponding to one of the limits of the miscibility gap (Parkhurst & Appelo, 2013). In such a case, AQ-TSS calculates the relative amounts of the two solids using a simple lever rule and displays a warning message at the end of the output file.

4.2. Nonregular Binary Solid Solutions: The Barite-Anglesite (Brt-Ang) Joint

The binary (Pb, Ba)SO$_4$ solid solution is nonideal, but the available nonideality parameters are mostly indirect, contradictory estimations. From statistics of natural occurrences, Glynn (2000) proposed a regular model with $a_0 = 2.7$, which implies the presence of a symmetric miscibility gap ($0.11 \lesssim X_{Brt} \lesssim 0.89$). However, other authors propose nonregular models, with a higher tolerance to the incorporation of lead into barite that results in an asymmetric miscibility gap. Moreover, studying the partitioning of minor amounts of lead in the barite-water system, some authors (Kolthoff & Noponen, 1938; McIntire, 1963; Zhu, 2004) proposed a regular model with a negative value of a_0 (≈ -1) and, therefore, a negative excess energy of mixing. Recently, Fernández-González et al. (2013) reconcile the contradiction between these different models from calorimetric measurements. According to these authors, there is a positive enthalpy of mixing for most of compositions, but such a tendency seems to be compatible with a negative anomaly for compositions very close to the barite end-member. The presence of negative values confirms the results obtained by Kolthoff and Noponen (1938) for trace concentrations of lead, but the

Table 2

Comparative Results Obtained for the Ideal and Regular Models of the (Ba, Sr)SO$_4$ Solid Solution ($a_0 = 2.3$, 298 K, 0.005 moles Brt, 0.0001 moles Clt, and 0.1 kg of Water)

Output	PHREEQC ideal	PHREEQC regular	AQ-TSS regular
$\left[Ba^{2+}\right]^T$	2.42E-06	9.69E-07	9.74E-07
$\left[Sr^{2+}\right]^T$	6.81E-05	2.08E-04	2.07E-04
X_{Brt}	0.982	0.984	0.984
X_{Clt}	0.018	0.016	0.016

Table 3
Comparative Results Obtained for the Nonideal Models of the (Ba, Pb)SO₄ Solid Solution (298 K, 0.005 moles Brt, 0.0001 moles Ang, and 0.1 kg of Water)

Output	PHREEQC subregular	AQ-TSS two regular ranges
$[Ba^{2+}]^T$	2.87E-06	2.82E-06
$[Pb^{2+}]^T$	5.65E-05	5.77E-05
X_{Brt}	0.9806	0.9815
X_{Ang}	0.0194	0.0185

Note. See text for details concerning the nonideality parameters.

uncertainty of the experimental data for this range of composition is very high. Here with the aim of testing AQ-TSS with a subregular binary solid solution, we use $a_0 = 2.409$ and $a_1 = -0.135$, which correspond to a slightly asymmetric gap ($0.142 < X_{Brt} < 0.808$) of miscibility. These values of a_0 and a_1 have been calculated by fitting the ΔG^E values reported by Fernández-González et al. (2013) to a Guggenheim expansion series of two terms. Figure 3a shows the corresponding $\Delta G^E(X_{Brt})$ curve.

In our implementation, we have combined two regular solution models, each one for a compositional range starting in one of the end-members. Figure 3a shows this subdivision of $\Delta G^E(X_{Brt})$, where the subregular function has been divided into:

(i) A regular $\Delta G^E(X_{Brt})$ function for the Ba-rich range, with $a_0 = 2.333$. Such a function represents a solid solution with a symmetric miscibility gap involving the range $0.142 \leq X_{Ang} \leq 0.858$, which is determined by the position of the two minima of the corresponding $\Delta G^M(X_{Ang})$ function (Figure 3b).

(ii) A regular $\Delta G^E(X_{Brt})$ model for the Pb-rich range, with $a_0 = 2.521$, which corresponds to a symmetric miscibility gap between 0.192 and 0.808, the two minima of the $\Delta G^M(X_{Brt})$ function (Figure 3b).

Table 3 displays a comparison between the outputs obtained using the PHREEQC tool for binary subregular solid solutions and AQ-TSS. The specific AQ-TSS program is included with the supporting information (for $cp < 10^{-5}$ convergence was attained after five iterations). Again, the difference between the data estimated by AQ-TSS and PHREEQC is negligible. Thus, by dividing the binary joints into several relevant ranges of composition we can apply AQ-TSS to complex solid solutions that do not fit with subregular models. It is worth noting that at the boundary between the two regular models ($X_{Brt} \approx 0.5$ in this case) there is a jump (see Figure 3a) in the value of mixing properties, which could be a source of inaccuracy. However, such a boundary falls within the miscibility gap (see Figure 3b). As explained in section 4.1, a solid with composition within this gap would be metastable would tend to recrystallize to form a mixture of solids with two compositions corresponding to the two limits of the miscibility gap ($X_{Brt} = 0.142$ and 0.808 in this example). In such a case, AQ-TSS calculates the relative amounts of the two solids and displays a warning message.

4.3. Comparison With GEMS and Experimental Results: Interaction of $Ra^{2+}_{(Aq)}$ With Barite

In order to check AQ-TSS, we have applied AQ-TSS and PHREEQC to reproduce some calculations performed by Vinograd et al. (2013) using GEMS (Kulik et al., 2013) and the NAGRA/PSI (Hummel et al., 2002) database. With this aim, we have calculated the equilibrium concentration of radium to which the system tends in the case of the interaction experiments of Curti et al. (2010), Bosbach et al. (2010), and Brandt et al. (2015). Table 4 shows the initial amounts of reactants, the calculated $\left[Ra^{2+}\right]^T$ values, and the experimental results obtained after prolonged interaction times. The AQ-TSS program for Curti et al. (2010) model is included with the supporting information, in all cases ($cp < 10^{-5}$) convergence was attained after four iterations. In all the three experimental series, the authors used SACHTLEBEN® barite, which consists of blocky crystals with a mean diameter of 10 μm and a specific surface area of 0.17 m² g⁻¹ (Klinkenberg et al., 2014).

As can be seen, the results obtained by AQ-TSS and PHREEQC are virtually equal. The results obtained using GEMS are of the same order of magnitude, the difference (∼5%) being reasonable given the different basis involved in both algorithms. There is also good agreement with the experimental results obtained by Bosbach et al. (2010) and Brandt et al. (2015), which seems to indicate that interaction times >400 days are required to approach equilibrium. Differently, the experiments by Curti et al. (2010) lasted 120 days and the final concentration is three or four times higher than the calculated values. As previously, stated, AQ-SS interactions involve ongoing dissolution-recrystallization and may need a long time to approach equilibrium.

5. Application to Ternary Systems

The testing performed with binary solid solutions supports the suitability of AQ-TSS to determine the state of thermodynamic equilibrium in AQ-SS systems. Now, the challenge is applying our implementation to

Table 4

Comparison of the Results Obtained Using AQ-TSS and PHREEQC to Determine the Equilibrium Concentration of Radium (Molality) in Experiments Performed by Curti et al. (2010)*,* Bosbach et al. (2010)*, and* Brandt et al. (2015)

Method		Curti et al.[a]	Bosbach et al.[b]	Brandt et al.[c]
Experimental		1.60E-09	1.10E-08	2.45E-09
GEMS		4.56E-10	1.17E-08	
AQ-TSS		4.33E-10	1.38E-08	2.71E-09
PHREEQC		4.33E-10	1.40E-08	2.73E-09
a	Reactants (moles)			
	Solid: $BaSO_4$ = 4.28E-04, solutes: $RaCl_2$ = 1.25E-08			
	Temperature: 298 K, time = 120 days, water = 1 kg			
b	Reactants (moles)			
	Solid: $BaSO_4$ = 2.14E-03, solutes: $RaCl_2$ = 3.00E-07; NaCl = 0.05; $NaNO_3$ = 0.5			
	Temperature = 293 K, time = 436 days, water = 1 kg			
c	Reactants (moles)			
	Solid: $BaSO_4$ = 3.64E-02, solutes: $RaBr_2$ = 5.00E-06			
	Temperature = 296 K, time = 443 days, water = 1 kg			

Note. The calculations were performed using a regular solid solution model with $a_0 = 1$ (Vinograd et al., 2013), the NAGRA/PSI (Hummel et al., 2002) database with $K_{RaSO_4} = 10^{-10.26}$. The equilibrium values obtained by Vinograd et al. (2013) using GEMS are also shown.

ternary solid solutions. With this aim, we have used the set of equations of section 3.3 to determine the activity-coefficient functions for ternary solid solutions. To simplify the formulations, we have divided the binary joints into several relevant composition ranges. Thus, subregular, binary solid solutions will be treated by combining two regular solid solution models. Ternary solid solutions will be treated by combining a set of regular models and neglecting ternary interactions, which represent a minor contribution when two of the three components occur in minor amounts. Such a scenario is realistic for ambient-temperature processes in which the host solid solutions exhibit wide miscibility gaps and the dissolved metal occurs in trace or minor amounts. We have chosen again sulfates of the barite family as case of study.

5.1. Interaction of $Pb^{2+}_{(Aq)}$ With Barite and Sr-Bearing Barite

Table 5 compiles the equilibrium states obtained by applying AQ-TSS to the interaction of 0.1 kg of a 0.1 millimolal $Pb(NO_3)$ aqueous solution with 0.0005 moles of solid solution. The PHREEQC file is attached with the supporting information ($cp < 10^{-5}$ convergence was attained after five iterations). Pure barite and four $(Ba, Sr)SO_4$ compositions with increasing Sr-content (0.05, 0.1, 0.15, and 0.2 X_{Clt}) were used as host solids. The corresponding AQ-TSS programs consider three binary joints with their specific nonideality models:

Anglesite-Barite Joint

The code combines two regular models by dividing the composition space into two ranges (see section 4.2.):

 i. A regular model for the Ba-rich range ($X_{Brt} > 0.5$), with $a_0 = 2.333$.
ii. A regular model for the Pb-rich range ($X_{Brt} < 0.5$), with $a_0 = 2.521$.

Table 5

Comparative Results Obtained for the Uptake of Pb by $(Ba, Sr)SO_4$ Solid Solutions (298 K, 0.0005 moles of SS, 0.00001 moles Aqueous Pb, and 0.1 kg of Water)

OUTPUT	$BaSO_4$	$Sr_{0.05}Ba_{0.95}SO_4$	$Sr_{0.1}Ba_{0.9}SO_4$	$Sr_{0.15}Ba_{0.85}SO_4$	$Sr_{0.2}Ba_{0.8}SO_4$
$[Ba^{2+}]^T$	1.19E-05	2.65E-06	1.23E-06	8.69E-07	7.15E-07
$[Pb^{2+}]^T$	1.05E-04	6.73E-05	3.44E-05	2.18E-05	1.54E-05
$[Sr^{2+}]^T$		1.00E-04	2.25E-04	3.12E-04	3.68E-04
X_{Brt}	0.992	0.972	0.948	0.918	0.880
X_{Ang}	0.008	0.025	0.034	0.038	0.040
X_{Clt}		0.003	0.018	0.044	0.080

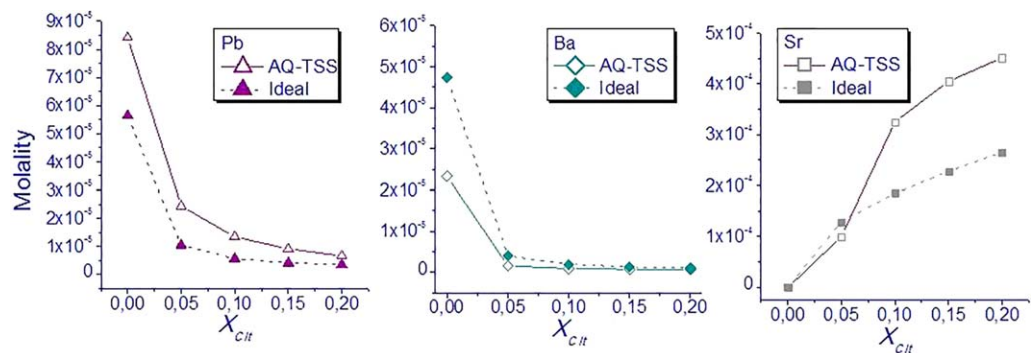*Note.* See text for details concerning the nonideality parameters. Concentrations in molalities.

Figure 4. Equilibrium concentration of Pb, Ba, and Sr after the interaction of $Pb^{2+}_{(aq)}$ with barite and Sr-bearing barite as a function of the celestine mole fraction in the parent solid solution. As can be seen, the decrease of concentration of lead (and barium) shows significant differences between both solid solution models.

Barite-Celestine Joint

A regular model with $a_0 = 2.3$ for the complete series (see section 4.1).

Anglesite-Celestine Joint

A regular model with $a_0 = -0.6515$ (Zhu, 2004). Such a model represents a solid solution with a strong tendency for lead to incorporate into the solid phase.

Inspection of Table 5 and Figure 4 shows that the higher the Sr-content in the host solid, the lower the equilibrium concentration of Pb in the aqueous solution. Vinograd et al. (2018) have also observed that trace amounts of $SrSO_4$ in the barite solid solution improves Ra-uptake. In practice, reaching equilibrium requires the parent solid to be completely dissolved and recrystallized, which maybe kinetically hindered. Anyhow, the calculations indicate a preferential tendency of lead to incorporate into the solid phase that agrees with previous experimental results (Prieto et al., 2016). This tendency is mainly due to both the lower solubility of anglesite in comparison with celestine and the negative value of the a_0 Guggenheim parameter favoring the formation of solid solution in the Sr-rich composition range. The influence of both parameters is clear considering the equilibrium partitioning of the substituting ions between the solid and the aqueous phase (e.g., Curti, 1997; Glynn & Reardon, 1990; Prieto, 2009). Using aqueous activities, for the binary anglesite-celestine system. the equilibrium distribution coefficient is given by:

$$D_{\frac{Ang}{Clt}(eq)} = \frac{\gamma_{Clt}}{\gamma_{Ang}} \times \frac{K_{Clt}}{K_{Ang}} \tag{22}$$

In which the quotient K_{Clt}/K_{Ang} of the solubility products is ≈ 14.5. The quotient $\gamma_{Clt}/\gamma_{Ang}$ of the solid-phase activity coefficients depends on the solid-solution composition, increasing for compositions in the Sr-rich range where it takes values ≈ 1.5. Therefore, both parameters are higher than unity, which involves preferential partitioning of lead toward the solid phase. Anyhow, the relevant point in here is comparing our results with those obtained using an ideal solid solution model. As can be observed in Figure 4, the estimated lead concentrations are significantly smaller using an ideal model. Therefore, the availability of implementations that work with nonideal ternary solid solutions is worthwhile.

6. Concluding Remarks

A rigorous treatment of nonideal multicomponent solid solutions requires using bulky formulations with numerous empirical parameters that are difficult, if not impossible, to determine. Moreover, many formulations are still under discussion, particularly those concerning ternary (or multiple) interactions between substituting ions. The simplest method to overcome this obstacle is using an ideal solid solution model as a first approximation. However, the aqueous concentrations of the substituting ions obtained in this way can significantly differ from the actual values. In a different way, AQ-TSS takes advantage of the "SOLID SOLUTIONS" tool incorporated in PHREEQC for ideal solid solutions. Using a relatively simple set of equations developed for regular solid solutions, AQ-TSS can deal with nonregular solid solutions by combining two or

even more regular models defined for specific ranges of composition for the corresponding binary joint. The treatment assumes that the contribution of ternary interactions is not very significant, which is realistic when two of the three components occur in minor amounts. AQ-TSS facilitates the study of the thermodynamic driving forces involved in aqueous-solid solution interactions. The actual behavior of these systems is determined by a combined effect of thermodynamic, kinetic, and mechanistic factors such as supersaturation, growth mechanisms and growth rates, presence of background electrolytes, competitive substitution, surface passivation, compositional zoning, etc. Geochemists frequently use correlations or semiempirical approaches to reveal the influence of these factors. Whereas empirical correlations can be useful for practical purposes, considering the equilibrium state to which the system tends is indispensable to understand the actual reaction pathways. In this framework, AQ-TSS can be a useful tool. An in depth evaluation of the presence of a third (or more) substituting ion on the partitioning behavior of the other two is, however, beyond the scope of this work. The lack of rigorous experimental data involving aqueous-ternary solid solution systems is a major obstacle and a challenge for our future research.

References

Allison, J. D., Brown, D. S., & Novo-Gradac, K. J. (1991). *MINTEQA2/PRODEFA2, a geochemical assessment model for environmental systems, version 3.0 user's manual* (Rep. EPA/600/3–91/021, pp. 107). Athens, GA: US Environmental Protection Agency.

Anderson, G. M. (2005). *Thermodynamics of natural systems* (2nd ed.). Cambridge, UK: Cambridge University Press.

Appelo, C. A. J., & Postma, D. (2005). *Geochemistry, groundwater and pollution* (pp. 649). Leiden, Netherlands: A.A. Balkema Publishers.

Bethke, C., & Yeakel, S. (2017). *The Geochemist's Workbench® release 11—GWB essentials guide* (pp. 117). Champaign, IL: Aqueous Solutions LLC.

Bosbach, D., Boettle, M., & Metz, V. (2010). *Experimental study on Ra²⁺ uptake by barite (BaSO₄). Kinetics of solid solution formation via BaSO₄ dissolution and RaₓBa₁₋ₓSO₄ (re)precipitation* (SKB Tech. Rep. TR-10–43). Stockholm, Sweden: Svensk Kärnbränslehantering AB.

Böttcher, M. E., & Dietzel, M. (2010). Metal-ion partitioning during low temperature precipitation of carbonates and sulphates. *EMU Notes Mineral*, *10*, 139–187. https://doi.org/10.1180/EMU-notes.10.4

Brandt, F., Curti, E., Klinkenberg, M., Rozov, K., & Bosbach, D. (2015). Replacement of barite by a (Ba, Ra)SO₄ solid solution at close-to-equilibrium conditions: A combined experimental and theoretical study. *Geochimica et Cosmochimica Acta*, *155*, 1–15. https://doi.org/10.1016/j.gca.2015.01.016

Bruno, J., Bosbach, D., Kulik, A., & Navrotsky, A. (2007). *Chemical thermodynamics of solid solutions of interest in nuclear waste management* (pp. 266). Paris, France: OCDE Nuclear Energy Agency Data Bank.

Curti, E. (1997). *Coprecipitation of radionuclides: Basic concepts, literature review and first applications* (PSI Rep. 97-10, pp. 107). Villigen, Switzerland: Paul Scherrer Institute.

Curti, E., Fujiwara, K., Iijima, K., Tits, J., Cuesta, C., Kitamura, A., et al. (2010). Radium uptake during barite recrystallization at 23 ± 2°C as a function of solution composition: An experimental ¹³³Ba and ²²⁶Ra tracer study. *Geochimica et Cosmochimica Acta*, *74*(12), 3553–3570. https://doi.org/10.1016/j.gca.2010.03.018

Fernández-González, A., Carneiro, J., Katsikopoulos, D., & Prieto, M. (2013). Thermodynamic properties of the (Ba, Pb)SO₄ solid solution under ambient conditions: Implications for the behavior of Pb and Ra in the environment. *Geochimica et Cosmochimica Acta*, *105*, 31–43. https://doi.org/10.1016/j.gca.2012.11.042

Ganguly, J. (2001). Thermodynamic modelling of solid solutions. *EMU Notes Mineral*, *3*, 37–69.

Ganguly, J., & Saxena, S. K. (1987). *Mixtures and mineral reactions* (pp. 289). Berlin, Germany: Springer-Verlag.

Glynn, P. (2000). Solid-solution solubilities and thermodynamics: Sulfates, carbonates and halides. *Reviews in Mineralogy and Geochemistry*, *40*(1), 481–511. https://doi.org/10.2138/rmg.2000.40.10

Glynn, P. D., & Reardon, E. J. (1990). Solid solution-aqueous solution equilibria: Thermodynamic theory and representation. *American Journal of Science*, *290*(2), 164–201. https://doi.org/10.2475/ajs.290.2.164

Glynn, P. D., Reardon, E. J., Plummer, L. N., & Busenberg, E. (1990). Reaction paths and equilibrium end-points in solid-solution aqueous-solution systems. *Geochimica et Cosmochimica Acta*, *54*(2), 267–282. https://doi.org/10.1016/0016-7037(90)90317-E

Godelitsas, A., & Astilleros, J. M. (2010). Dissolution, sorption/(re)precipitation, formation of solid solutions and crystal growth phenomena on mineral surfaces: Implications for the removal of toxic metals from the environment. *EMU Notes Mineral*, *10*, 289–324. https://doi.org/10.1180/EMU-notes.10.8

Guggenheim, E. A. (1937). Theoretical basis of Raoult's law. *Transactions of the Faraday Society*, *33*, 151–159. https://doi.org/10.1039/tf9373300151

Hanor, J. F. (2000). Barite-celestine geochemistry and environments of formation. *Reviews in Mineralogy and Geochemistry*, *40*(1), 193–276. https://doi.org/10.2138/rmg.2000.40.4

Hillert, M. (1980). Empirical methods of predicting and representing thermodynamic properties of ternary solution phases. *Calphad*, *4*(1), 1–12. https://doi.org/10.1016/0364-5916(80)90016-4

Hummel, W., Berner, U., Curti, E., Pearson, F. J., & Thoenen, T. (2002). *Nagra/PSI chemical, thermodynamic data base 01/01*, (Nagra Tech. Rep. NTB 02–16). Wettingen, Switzerland: Nagra. ISBN 1–58112-620–624

Katsikopoulos, D., Fernández-González, A., & Prieto, M. (2009). Precipitation and mixing properties of the "disordered" (Mn, Ca)CO₃ solid solution. *Geochimica et Cosmochimica Acta*, *73*(20), 6147–6161. https://doi.org/10.1016/j.gca.2009.07.001

Klinkenberg, M., Brandt, F., Breuer, U., & Bosbach, D. (2014). Uptake of Ra during the recrystallization of barite: A microscopic and time of flight-secondary ion mass spectrometry study. *Environmental Science & Technology*, *48*(12), 6620–6627. https://doi.org/10.1021/es405502e

Kolthoff, I. M., & Noponen, G. E. (1938). Studies on aging of fresh precipitates. XVII. The equilibrium between mixed crystals of barium-lead sulfate solutions. *Journal of the American Chemical Society*, *60*(1), 39–201. https://doi.org/10.1021/ja01268a010

Kulik, D. A., Vinograd, V., Paulsen, N., & Winkler, B. (2010). (Ca, Sr)CO₃ aqueous-solid solution systems: From atomistic simulations to thermodynamic modeling. *Physics and Chemistry of the Earth*, *35*(6–8), 217–232. https://doi.org/10.1016/j.pce.2010.04.011

Kulik, D. A., Wagner, T., Dmytrieva, S. V., Kosakowski, G., Hingerl, F. F., Chudnenko, K. V., et al. (2013). GEM-Selektor geochemical modeling package: Revised algorithm and GEMS3K numerical kernel for coupled simulation codes. *Computational Geosciences*, *17*, 1–24. https://doi.org/10.1007/s10596-012-9310-6

McIntire, W. L. (1963). Trace element partition coefficients—A review and application to geology. *Geochimica et Cosmochimica Acta*, *27*(12), 1209–1264. https://doi.org/10.1016/0016-7037(63)90049-8

Monnin, C., & Cividini, D. (2006). The saturation state of the world's ocean with respect to (Ba, Sr)SO₄ solid solutions. *Geochimica et Cosmochimica Acta*, *70*(13), 3290–3298. https://doi.org/10.1016/j.gca.2006.04.002

Mucci, A. (2004). The behavior of mixed Ca-Mn carbonates in water and seawater: Controls of manganese concentration in marine porewaters. *Aquatic Geochemistry*, *10*(1/2), 139–121. https://doi.org/10.1023/B:AQUA.0000038958.56221.b4

Mukhopadhyay, B., Basu, S., & Holdaway, M. J. (1993). A discussion of Margules-type formulations for multicomponent solid solutions with a generalized approach. *Geochimica et Cosmochimica Acta*, *57*(2), 277–283. https://doi.org/10.1016/0016-7037(93)90430-5

Noguera, C., Fritz, B., & Clément, A. (2012). A theoretical treatment of the precipitation of doubly substituted solid solutions in aqueous solutions. *Crystal Growth & Design*, *12*(7), 3444–3457. https://doi.org/10.1021/cg201621s

Parkhurst, D. L., & Appelo, C. A. J. (2013). *Description of input and examples for PHREEQC version 3—A computer program for speciation, batch-reaction, one-dimensional transport, and inverse geochemical calculations* (book 6). Washington DC: U.S. Geological Survey Techniques and Methods.

Prieto, M. (2009). Thermodynamics of solid solution-aqueous solution systems. *Reviews in Mineralogy and Geochemistry*, *70*(1), 47–85. https://doi.org/10.2138/rmg.2009.70.2

Prieto, M., Astilleros, J. M., & Fernández-Díaz, L. (2013). Environmental remediation by crystallization of solid solutions. *Elements*, *9*(3), 195–201. https://doi.org/10.2113/gselements.9.3.195

Prieto, M., Heberling, F., Rodríguez-Galán, R., & Brandt, F. (2016). Crystallization behavior of solid solutions from aqueous solutions: An environmental perspective. *Progress in Crystal Growth and Characterization of Materials*, *62*(3), 29–68. https://doi.org/10.1016/j.pcrysgrow.2016.05.001

Putnis, A. (2010). Effects of kinetics and mechanism of crystal growth on ion-partitioning in solid solution-aqueous solution (SS-AS) systems. Ion partitioning in ambient-temperature aqueous systems. *EMU Notes Mineral*, *10*, 43–64. https://doi.org/10.1180/EMU-notes.10.2

Putnis, A., Fernández-Díaz, L., & Prieto, M. (1992). Experimentally produced oscillatory zoning in the (Ba, Sr)SO₄ solid solution. *Nature*, *358*(6389), 743–745. https://doi.org/10.1038/358743a0

Thompson, J. B., & Waldbaum, D. (1969). Analyses of the two-phase region halite-sylvite in the system NaCl-KCl. *Geochimica et Cosmochimica Acta*, *33*(6), 671–690. https://doi.org/10.1016/0016-7037(69)90114-8

Vinograd, V. L., Brandt, F., Rozov, K., Klinkenberg, M., Refson, K., Winkler, B., et al. (2013). Solid-aqueous equilibrium in the BaSO₄-RaSO₄-H₂O system: First-principles calculations and a thermodynamic assessment. *Geochimica et Cosmochimica Acta*, *122*, 398–417. https://doi.org/10.1016/j.gca.2013.08.028

Vinograd, V. L., Kulik, D. A., Brandt, F., Klinkenberg, M., Weber, J., Winkler, B., et al. (2018). Thermodynamics of the solid solution-aqueous solution system (Ba, Sr, Ra)SO₄ + H₂O: I. The effect of strontium content on radium uptake by barite. *Applied Geochemistry*, *89*, 59–74. https://doi.org/doi.org/10.1016/j.apgeochem.2017.11.009

Vinograd, V. L., Paulse, N., Winkler, B., & van de Walle, A. (2010). Thermodynamics of mixing in the ternary rhombohedral carbonate solid solution, CaxMgyMn₁-x-yCO₃, from atomistic simulations. *Calphad*, *34*(1), 113–119. https://doi.org/10.1016/j.calphad.2010.01.002

Wagner, T., Kulik, D. A., Hingerl, F. F., & Dmytrieva, S. V. (2012). GEM-Selektor geochemical modeling package: TSolMod library and data interface for multicomponent phase models. *The Canadian Mineralogist*, *50*(5), 1173–1195. https://doi.org/10.3749/canmin.50.5.1173

Wang, Q., Grau-Crespo, R., & de Leeuw, N. (2011). Mixing thermodynamics of the calcite-structured (Mn,Ca)CO₃ solid solution: A computer simulation study. *Journal of Physical Chemistry*, *115*(47), 13854–13861. https://doi.org/10.1021/jp200378q

Wolery, T. J. (1992). *EQ3/6, a software package for geochemical modeling of aqueous systems* (Rep. UCRL-MA-110662 Pt-I-III, 246 pp.). Livermore, CA: Lawrence Livermore National Laboratory.

Zhang, T., Gregory, K. W., Hammack, R., & Vidic, R. D. (2014). Co-precipitation of radium with barium and strontium sulfate and its impact on the fate of radium during treatment of produced water from unconventional gas extraction. *Environmental Science & Technology*, *48*(8), 4596–4603. https://doi.org/10.1021/es405168b

Zhu, C. (2004). Coprecipitation in the barite isostructural family: 1. Binary mixing properties. *Geochimica et Cosmochimica Acta*, *68*(16), 3327–3337. https://doi.org/10.1016/j.gca.2003.10014